

# Field Trial Results on Different Uplink Coordinated Multi-Point (CoMP) Concepts in Cellular Systems

Patrick Marsch, Michael Grieger, Gerhard Fettweis  
Technische Universität Dresden, Vodafone Chair Mobile Communications Systems,  
01069 Dresden, Germany  
Email: {marsch, michael.grieger, fettweis}@ifn.et.tu-dresden.de

**Abstract**—Coordinated multi-point (CoMP) in the cellular uplink appears to be an effective option to combat inter-cell interference, offering large improvements in spectral efficiency and fairness. However, one major drawback of these schemes is that they typically require a large extent of additional backhaul infrastructure compared to a non-cooperative system. A large amount of theoretical work has been published on this topic, emphasizing the benefit of adapting between different CoMP strategies depending on the channel realization in order to optimize the rate/backhaul trade-off. This paper complements previous publications through field trial results obtained in a representative urban setup. The results yield an insight into practical issues connected to some schemes, while being fairly correlated to theoretical predictions and in fact further emphasizing the gain of adaptive CoMP.

## I. INTRODUCTION

As the demand for higher transmission rates and spectral efficiency in cellular mobile communication systems is steadily increasing, a reuse of radio resources in every cell is desired. Nonetheless, the occurring inter-cell interference is not sufficiently addressed in LTE Release 8 [1], leading to a strong performance degradation especially for cell-edge users. In previous work, it has been shown that a potential solution to the inter-cell interference problem is given by a coordinated reception or transmission. These coordinated multi-point (CoMP) techniques are shown to yield large spectral efficiency and fairness gains [2], [3]. However, the technical challenges of CoMP implementations are manifold. Prominent examples are the synchronization of all cooperating entities in time and frequency [4], multi-cell channel estimation [5], and backhaul-efficient multi-cell signal processing [6], [7]. Even though significant achievements have been attained, the isolated examination of a certain problem is not sufficient to prove the maturity of the ambitious CoMP concepts. To this end, the potential performance of CoMP and the corresponding system complexity need to be assessed under real-world conditions, i.e. through field trials as conducted in the EASY-C project [8].

In previous work [9], we presented measurement results for a cellular uplink where two terminals (UEs) were jointly detected by two cooperating base stations (BSs). We here observed a distributed antenna system (DAS), assuming that one BS forwards compressed receive signals to the other, where decoding of both UEs took place. In the cited work, we did not consider the required backhaul, but in a practical system, this can be a severe issue [10]. From theory,

it is known that the backhaul requirement can be strongly reduced through different CoMP concepts. In particular, the BSs may exchange decoded information bits for the purpose of interference cancellation, a method that was already shown to be very backhaul efficient from an information theoretical point of view in [11], where the concept is referred to as distributed interference subtraction (DIS). Theoretical results further show that the performance of different cooperation schemes strongly depends on the particular channel. Field trial measurements allow to identify characteristic channel scenarios and observing the achievable performance. In particular, we are interested how this measured performance compares with theoretical predictions.

The paper is organized as follows. In Section II, we provide a short overview of our measurement setup. The signal processing architecture which includes cooperative and non-cooperative detection is addressed in Section III. Information theoretic rate bounds are stated in Section IV, which are subsequently compared to field trial results in Section V. The paper is concluded in Section VI.

## II. MEASUREMENT SETUP

As shown in Figure 1, the measurement setup consists of two BSs deployed on the rooftop of a building in Dresden, spaced by about 150 m. The BSs are synchronized through GPS fed reference normals and connected through a microwave link. Each BS is equipped with a cross-polarized directional antenna (70 degrees half-power beamwidth, 14 dBi gain), hence with  $N_{\text{bs}} = 2$  individual antenna elements per BS. The UEs - employing one omnidirectional antenna each - transmit using OFDM and a sequence of different modulation and coding schemes (MCSs), as listed in Table II. Both UEs are scheduled to transmit on the same resource in time and frequency. In general, the BS receive signals are recorded for offline evaluation, as this facilitates the implementation and test of different detection concepts. Various transmission parameters are listed in Table I.

## III. SIGNAL PROCESSING ARCHITECTURE

In the next subsections, we will briefly explain the general signal processing steps performed in our architecture. For a more thorough discussion, we refer to [9].

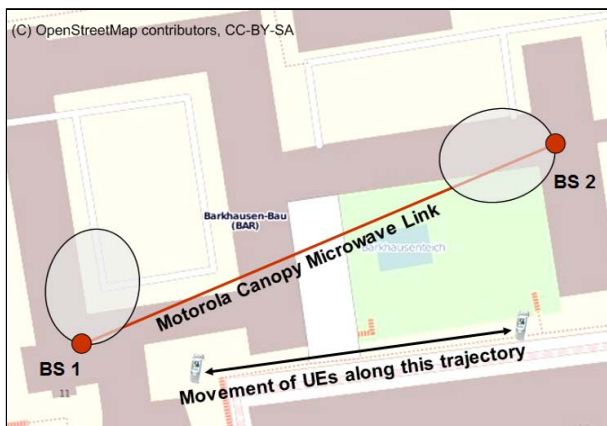


Fig. 1: Measurement setup.

Carrier frequency	2.53 GHz
System bandwidth	10 MHz
Resource blocks (PRBs)	30
No. of sub-carriers per PRB	12
Transmit Power	-5 dBm
Quantization resolution	6 or 12 bit per real dim.

TABLE I: Transmission parameters

### A. Synchronization

The carrier frequency of the BSs is synchronized by using GPS fed reference normals. As shown in [12], remaining synchronization errors can be neglected in the uplink. On the UE side, the frequency offset is precompensated using downlink reference signals. Compared to the subcarrier spacing, the remaining frequency offset of about 200 Hz is small enough to disregard co-channel interference. The common phase error (CPE) is taken into account by an appropriate interpolation of channel estimates.

### B. Channel and Noise Covariance Estimation

The channel is estimated by a pilot based approach using the LTE pilot positions. Interference between pilot symbols of different UEs is avoided by a code orthogonal design using Frank-Zadoff-Chu sequences. Due to a spreading factor of two, the channel is estimated for every second sub-carrier in the frequency domain. In order to estimate the channel for all other sub-carriers, time and frequency interpolation are carried out separately. Note that the estimated channel links inherently contain the transmit power. The noise covariance is estimated based on the channel estimates. In particular, we exploit the autocorrelation properties of the estimated channel to separate its noise and signal components and determine one noise variance estimate per BS.

### C. Channel Equalization

If residual synchronization errors are neglected and we assume a flat channel on each sub-carrier of bandwidth  $\Delta F = 15$  kHz, the transmission of each symbol on a single sub-carrier

of the OFDM system can be stated as

$$\begin{aligned} \mathbf{y}_1 &= \mathbf{h}_{1,1}x_1 + \mathbf{h}_{1,2}x_2 + \mathbf{n}_1, \\ \mathbf{y}_2 &= \mathbf{h}_{2,1}x_1 + \mathbf{h}_{2,2}x_2 + \mathbf{n}_2, \end{aligned} \quad (1)$$

where  $\mathbf{y}_m \in \mathbb{C}^{[N_{\text{bs}} \times 1]}$  are the signals received by the  $N_{\text{bs}}$  antennas of BS  $m$ ,  $\mathbf{h}_{m,n} \in \mathbb{C}^{[N_{\text{bs}} \times 1]}$  denotes the channel gain matrix from UE  $n$  to BS  $m$ ,  $x_n \in \mathbb{C}$  is a symbol transmitted by UE  $n$ , and  $\mathbf{n}_m \in \mathbb{C}^{[N_{\text{bs}} \times 1]}$  denotes additive, uncorrelated noise of covariance  $E\{\mathbf{n}_m \mathbf{n}_m^H\} = \sigma_m^2 \mathbf{I}$ . The channel vectors include UE transmit power, hence  $E\{x_n x_n^H\} = 1$ .

The signal processing architecture enables a variety of equalization schemes connected to different CoMP strategies, of which the following examples are illustrated in Fig. 2:

- Both UEs can be decoded individually by their assigned BS (see Fig. 2a), possibly with a swapped BS-UE assignment (see Fig. 2b).
- Both UEs can be decoded by the same BS, possibly using successive interference cancellation (SIC, see Fig. 2c).
- Both UEs can be decoded individually by their assigned BSs, but one BS forwards decoded data bits to another for distributed interference cancellation (DIS, see Fig. 2d).
- One BS compresses and forwards all received signals to the other BS, where both UEs are decoded (denoted DAS). This can be done via linear equalization (see Fig. 2e), possibly in conjunction with SIC (see Fig. 2f).

Equalization itself is generally based on linear MMSE filters, which depend on whether any kind of interference subtraction (i.e. through DIS or SIC) has been performed in advance. If UE  $n$  is locally detected at BS  $m$ , and still subject to the interference from UE  $\bar{n} \neq n$ , the biased MMSE filter for a particular subcarrier is given as

$$\mathbf{G}_{\text{biased}}^{[m,n]} = \hat{\mathbf{h}}_{m,n}^H \left( \hat{\mathbf{h}}_{m,n} \hat{\mathbf{h}}_{m,n}^H + \hat{\mathbf{h}}_{m,\bar{n}} \hat{\mathbf{h}}_{m,\bar{n}}^H + \hat{\sigma}_m^2 \mathbf{I} \right)^{-1}, \quad (2)$$

where  $\hat{\mathbf{h}}$  and  $\hat{\sigma}_m^2$  are estimates of the channel and noise, respectively, and  $\bar{n}$  is the index of the interfering UE. Note that this implementation exploits the channel knowledge to each UE for the purpose of interference rejection combining. If the receive signal of both BSs are available at a joint receiver, the biased MMSE filter for UE  $n$  is given as

$$\mathbf{G}_{\text{biased}}^{[n]} = \hat{\mathbf{h}}_n^H \left( \hat{\mathbf{h}}_n \hat{\mathbf{h}}_n^H + \hat{\mathbf{h}}_{\bar{n}} \hat{\mathbf{h}}_{\bar{n}}^H + \begin{bmatrix} \hat{\sigma}_1^2 \mathbf{I} & 0 \\ 0 & \hat{\sigma}_2^2 \mathbf{I} \end{bmatrix} \right)^{-1}, \quad (3)$$

where  $\hat{\mathbf{h}}_n = [\hat{\mathbf{h}}_{1,n}^T \ \hat{\mathbf{h}}_{2,n}^T]^T$ . If interference of the other UE has already been canceled, filters in (2), (3) change to

$$\mathbf{G}_{\text{SIC/DIS,based}}^{[m,n]} = \hat{\mathbf{h}}_{m,n}^H \left( \hat{\mathbf{h}}_{m,n} \hat{\mathbf{h}}_{m,n}^H + \hat{\sigma}_m^2 \mathbf{I} \right)^{-1} \quad (4)$$

$$\text{and } \mathbf{G}_{\text{SIC,based}}^{[n]} = \hat{\mathbf{h}}_n^H \left( \hat{\mathbf{h}}_n \hat{\mathbf{h}}_n^H + \begin{bmatrix} \hat{\sigma}_1^2 \mathbf{I} & 0 \\ 0 & \hat{\sigma}_2^2 \mathbf{I} \end{bmatrix} \right)^{-1}, \quad (5)$$

respectively. In order to avoid an increased bit error probability for higher order modulation schemes, the bias has to be removed from all previously stated filters, i.e. we apply

$$\mathbf{G} = (\Delta(\mathbf{G}_{\text{biased}}))^{-1} \mathbf{G}_{\text{biased}}, \quad (6)$$

where  $\Delta(\mathbf{A})$  sets all off-diagonal elements of  $\mathbf{A}$  to zero.

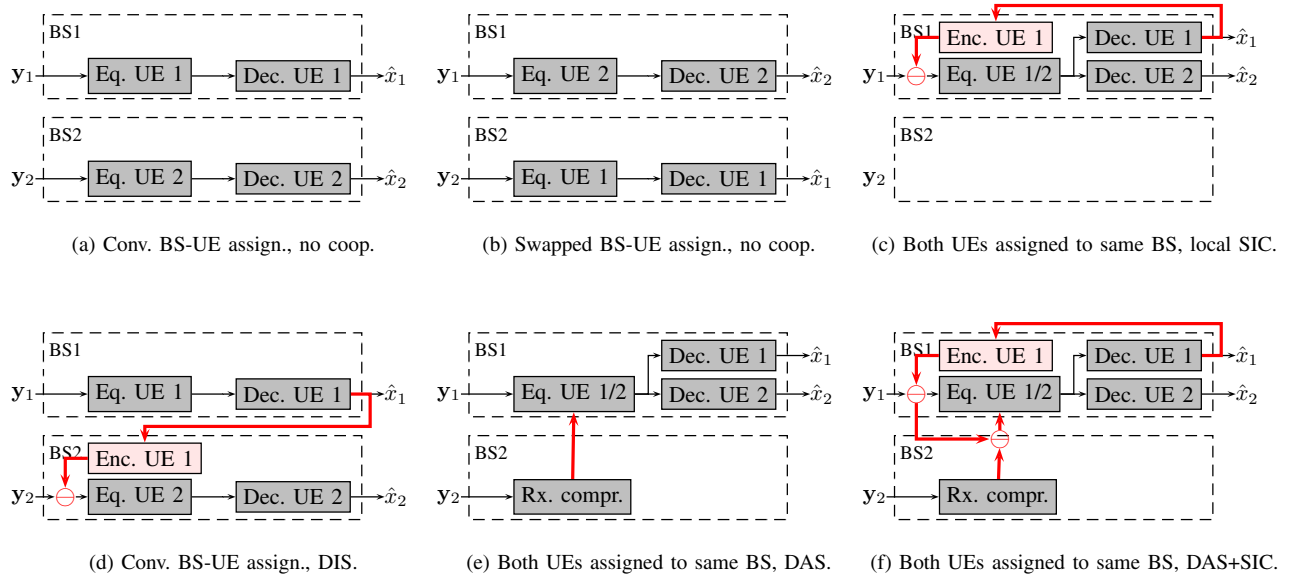


Fig. 2: Signal processing setup for various exemplary detection / cooperation schemes.

MCS#	Mod. scheme	Code rate	Peak rate	Bit per channel use
1	4QAM	2/3	4.54 Mbps	1.34
2	16QAM	1/2	6.91 Mbps	2.00
3	16QAM	2/3	9.29 Mbps	2.66
4	16QAM	3/4	10.6 Mbps	3.00
5	16QAM	6/7	12.3 Mbps	3.43

TABLE II: Modulation schemes and code rates used for transmission, assuming turbo codes as used in LTE Rel. 8.

#### D. Soft Demodulation and Decoding

After equalization, signal-to-interference-and-noise ratios (SINRs) are estimated via an error vector magnitude approach [13], followed by soft demodulation. The demodulator output is fed into an LTE Rel. 8 compliant decoding chain using the codes listed in Table II. Each codeword spans one transmit time interval (TTI) in time domain and 30 physical resource blocks (PRBs) in frequency domain. Decoding success is determined through an outer CRC-code.

#### E. Interference Cancellation

In this work, we only consider hard-SIC after successful decoding, which can be performed locally at one BS, or remotely, if decoded data is handed over the backhaul. In general, decoded bits connected to one UE are re-encoded, re-modulated, multiplied with the estimated channel, and then subtracted from the received signals (see Figs. 2c, 2d and 2f).

#### F. Received Signal Compression

In the case where one BS compresses all received signals and forwards these to the other, we here assume that each involved symbol in frequency domain is compressed with a linear quantizer either employing 6 or 12 bits per receive

antenna and real signal dimension. Clearly, more sophisticated quantization approaches and/or source coding could be applied as considered in [14], but we leave this for future field trials.

#### IV. RATE BOUNDS FROM INFORMATION THEORY

We now state analytical expressions for inner bounds on rates that can be achieved under a given channel realization and a particular cooperation and equalization scheme. We model the channel estimate available at the BS side as

$$\hat{\mathbf{H}} = \mathbf{H} + \mathbf{E}, \quad (7)$$

where the error  $\mathbf{E} \in \mathbb{C}^{[2N_{\text{bs}} \times 2]}$  is a random variable with

$$E \{ \text{vec}(\mathbf{E}) \text{vec}(\mathbf{E})^H \} = \frac{\sigma_{\text{pilots}}^2}{N_p \cdot p_{\text{pilots}}} \cdot \mathbf{I} = \sigma_E^2 \cdot \mathbf{I}. \quad (8)$$

Equation (8) is based on the Kramer-Rao lower bound [15], yielding the absolute estimation error variance if optimal channel estimation has been performed based on  $N_p$  pilots of power  $p_{\text{pilots}}$ , subject to Gaussian noise with variance  $\sigma_{\text{pilots}}^2$ . In the sequel, we assume unit-power pilots ( $p_{\text{pilots}} = 1$ ), and choose  $N_p = 2$ , which has been motivated by the observation of a concrete 2D MMSE channel estimation scheme in a frequency-selective OFDMA system for a channel with urban delay spread and pedestrian UE speed in [16]. It has further been shown that we can lower-bound the performance of a transmission as in (1) under imperfect channel knowledge by observing the modified transmission equation

$$\mathbf{y} = \mathbf{H}^e \mathbf{x} + \mathbf{v} + \mathbf{n}, \quad (9)$$

with a power-reduced effective channel  $\mathbf{H}^e \in \mathbb{C}^{[2N_{\text{bs}} \times 2]}$  with

$$\forall i, j: \quad h_{i,j}^e = \frac{h_{i,j}}{\sqrt{1 + \sigma_E^2 / E \{ |h_{i,j}|^2 \}}}, \quad (10)$$

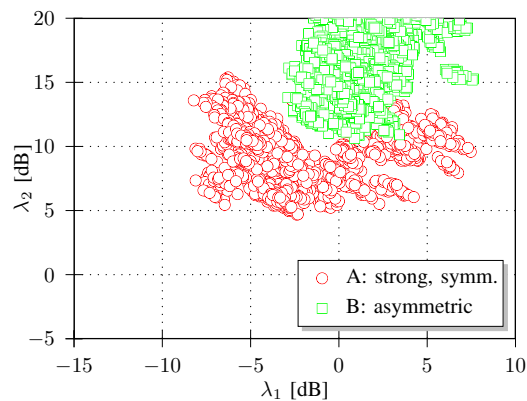


Fig. 3: Interference scenarios discussed in this paper.

and an additional Gaussian noise term  $\mathbf{v} \in \mathbb{C}^{[2N_{\text{bs}} \times 1]}$  with

$$E\{\mathbf{v}\mathbf{v}^H\} = \Phi^{\text{vv}} = \Delta \left( \bar{\mathbf{E}}^e (\bar{\mathbf{E}}^e)^H \right), \quad (11)$$

$$\text{where } \forall i, j : \bar{e}_{i,j}^e = \sqrt{\frac{E\{|h_{i,j}|^2\} \cdot \sigma_E^2}{E\{|h_{i,j}|^2\} + \sigma_E^2}}. \quad (12)$$

The derivation is stated in [14], [17]. Analog to the filters described in (2)-(5), we can now lower-bound the rate of UE  $n$  decoded by BS  $m$  and interfered by UE  $\bar{n}$  as

$$R_n^m \leq \log_2 \left| \mathbf{I} + \left( \mathbf{h}_{m,\bar{n}}^e (\mathbf{h}_{m,\bar{n}}^e)^H + \Phi_m^{\text{vv}} + \sigma_m^2 \mathbf{I} \right)^{-1} \mathbf{h}_{m,n}^e (\mathbf{h}_{m,n}^e)^H \right|, \quad (13)$$

where the channels as usual contain the UE transmit powers, and  $\Phi_m^{\text{vv}}$  is the submatrix of  $\Phi^{\text{vv}}$  connected to BS  $m$ . All other rates (for joint decoding by both BSs after the usage of DAS concepts, or after interference cancellation), can be derived equivalently, and are omitted here for brevity.

### V. COMPARISON OF THEOR. AND MEASURED RATES

We initially compare the terminal rates that should be achievable according to information theory to rates actually measured in the field trial described in Section II. The information theoretic numbers are computed for each 12th sub-carrier and each 7th OFDM symbol, using the channel coefficients and noise levels estimated from the field trial results.

For rate expressions based on actual transmissions, we collect statistics for the 5 different MCSs stated in Table II. For each transmission of 20 TTIs, we then determine the MCS that has led to the highest number of successfully transmitted bits, and translate this into an average number of bits per channel use. This hence reflects ideal link adaptation. Still, practically achieved rates are significantly lower than those based on information theory, as the former are constrained through a very limited set of MCSs and are deteriorated due to practical block lengths and various RF impairments.

We have done measurements for various UE locations, yielding a variety of interference scenarios. To characterize these, we introduce terms  $\lambda_1$  and  $\lambda_2$  stating the ratio of the average channel gain of a UE to its assigned BS over the

average channel gain to the other BS, for UEs 1 and 2, respectively. A large value means that a UE has a stronger link to its own BS than to the other one, while a value of 0 dB corresponds to the cell-edge case. From the  $\lambda$  values measured and shown in Fig. 3, we have identified two clusters of interference scenarios to be observed in the sequel:

- **A:** Scenarios of strong, almost symmetrical interference
- **B:** Scenarios of highly asymmetrical interference

The plots in Fig. 4 show the cumulative distribution functions of UE rates, connected to theoretical (solid lines) or practical (dashed lines) performance. Gray curves denote a fixed BS-UE assignment (based on long-term average path-loss) and no BS cooperation. Black lines indicate the performance if a flexible BS-UE assignment on TTI basis is used, where filled markers denote the option of decoding both UEs at the same BS with local SIC. Blue lines indicate the DIS concept, and red lines DAS concepts with 6 or 12 quantization bits per antenna and real signal dimension, where we distinguish between MMSE (hollow markers) and SIC (filled markers).

In Plot 4a, for fairly symmetrical interference (scen. A) and  $N_{\text{bs}}=1$ , we see a theoretical gain of local, non-cooperative SIC, and a further rate increase of DIS (A), but all schemes are inferior to DAS. In the latter case, SIC appears highly beneficial (B), as the compound channel matrix is often rank-deficient. Practical results reflect this, except that interference cancellation gains (DIS or DAS+SIC) are reduced (C). This is due to the limited granularity of MCSs, and the fact that interference cancellation is strongly subject to error propagation if interference links cannot be estimated well. Plot 4b shows the same interference scenario for  $N_{\text{bs}}=2$ . Here, fast fading dependent BS-UE assignment is beneficial (D), as the system offers more spatial degrees of freedom not reflected by average path losses. The superiority of DAS now increases, as array gain becomes the main source of CoMP gain, while local IRC reduces effective interference. The difference between linear and non-linear decoding is now minimal, as the 4x2 compound channel already yields sufficient orthogonality. Practical results reflect all theoretical observations quite well, except that the small gain of DAS+SIC over DAS disappears (E).

Plots 4c and 4d consider highly asymmetrical interference (scen. B), where UE 1 is near the cell edge and UE 2 close to its cell-center. With  $N_{\text{bs}}=1$ , DIS concepts are highly beneficial for UE 2, as BS 1 can decode UE 1 almost free of interference, and forward the corresponding data bits to BS 2 for effective interference subtraction. In theory, the performance almost reaches that of centralized DAS, but in practice, the DIS concept obtains only about 50% of the predicted gain (F). Still, this scheme is highly attractive in terms of backhaul, as we will see later. For  $N_{\text{bs}}=2$ , local decoding without BS cooperation becomes more attractive, as a large extent of interference can be mitigated through interference rejection combining. Still, DIS schemes are attractive for UE 2, with a particular benefit in terms of outage improvement. This is also reflected in practice (G), though the gains of DAS+SIC over DAS are again too marginal to be visible here.

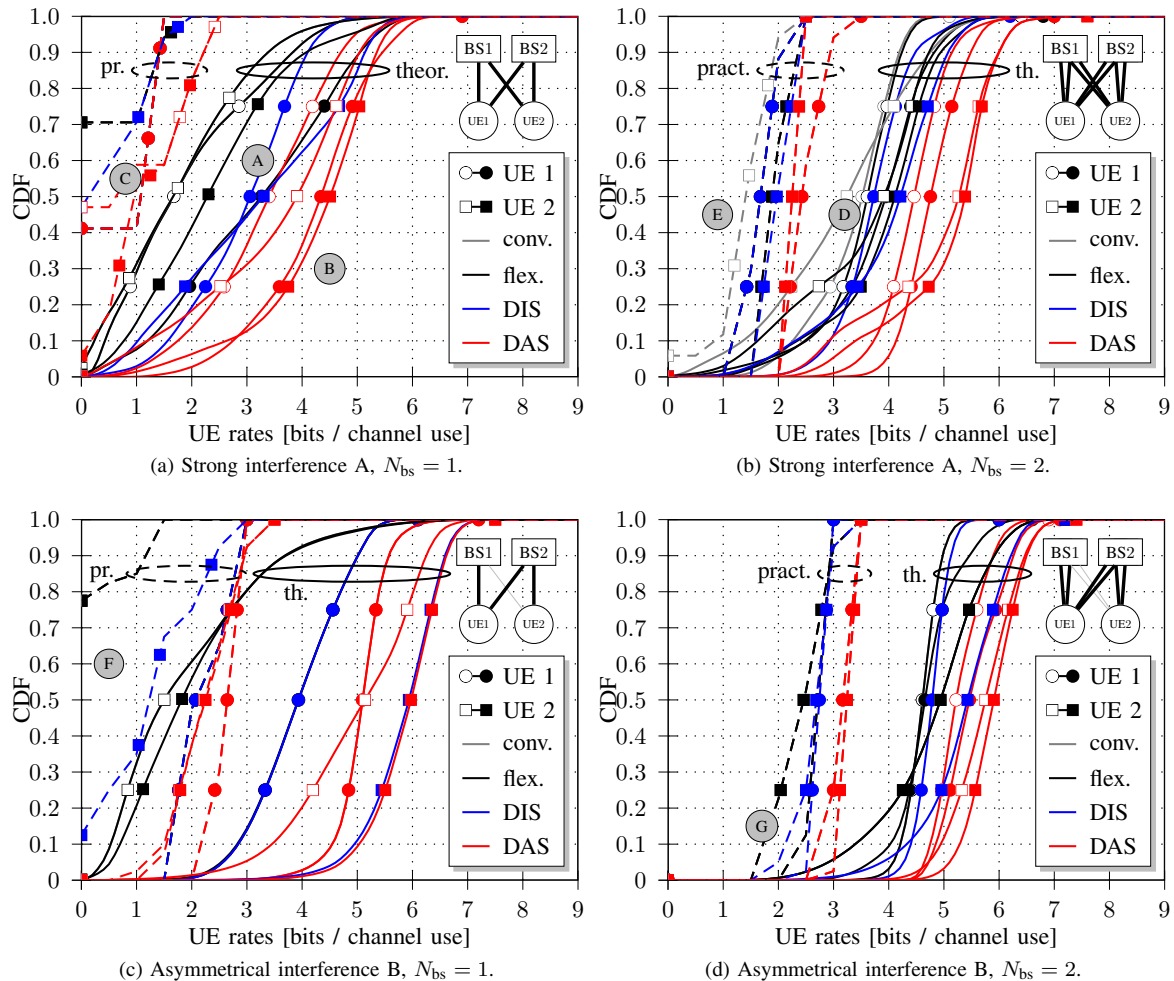


Fig. 4: Theoretical and measured UE rates.

In Fig. 5, we finally investigate the trade-off between rates and required backhaul for the practical transmission results for the same scenarios discussed before. We here distinguish between DAS concepts using 6 or 12 quantization bits per receive antenna and real signal dimension. Note that for each TTI, we only consider the backhaul required for DIS and DAS concepts if these actually improve decoding success. As 12 bit quantization leads to success much more often than the other case, the difference in required *average* backhaul may be a factor much larger than 2. For symmetric interference and  $N_{bs}=1$ , the before mentioned performance gain of using SIC on top of DAS is hence also accompanied by an increase in required backhaul (H). We see that there is limited gain of using DIS (while being very backhaul-efficient), except for asymmetric interference and in particular for  $N_{bs} = 1$ , where DIS provides more than 50% of the possible CoMP gain for UE 2, outperforming DAS with 6 quant. bits, while requiring about 20 times less backhaul than DAS with 12 bits (I). The results hence emphasize the benefit of fast-fading dependent BS-UE assignment and adaptive CoMP, which was previously suggested in theoretical work in, e.g., [11], [14].

## VI. CONCLUSIONS AND OUTLOOK

We have investigated different BS cooperation concepts for uplink CoMP w.r.t. the achievable rate/backhaul trade-off. For a setup with two BSs and two UEs, we have tested these concepts under practical signal propagation conditions, and compared the achieved rates to those expected from theory, given the measured channel realizations. Theoretical and practical observations correlate well in the way that decentralized CoMP schemes based on an exchange of decoded user data between BSs are best suitable for asymmetric interference, but can generally only offer a limited extent of CoMP gain. The practical results furthermore reveal that the gain from decentralized schemes is smaller than expected, but the difference in backhaul requirements between decentralized and centralized schemes is significantly larger, and hence pronounces the benefit of adaptive, interference-dependent CoMP. Currently, research is being done on improved (vector) quantization techniques for DAS, and measurements are taking place in the EASY-C test bed in downtown Dresden where the gains of (adaptive) uplink CoMP are investigated over larger areas.

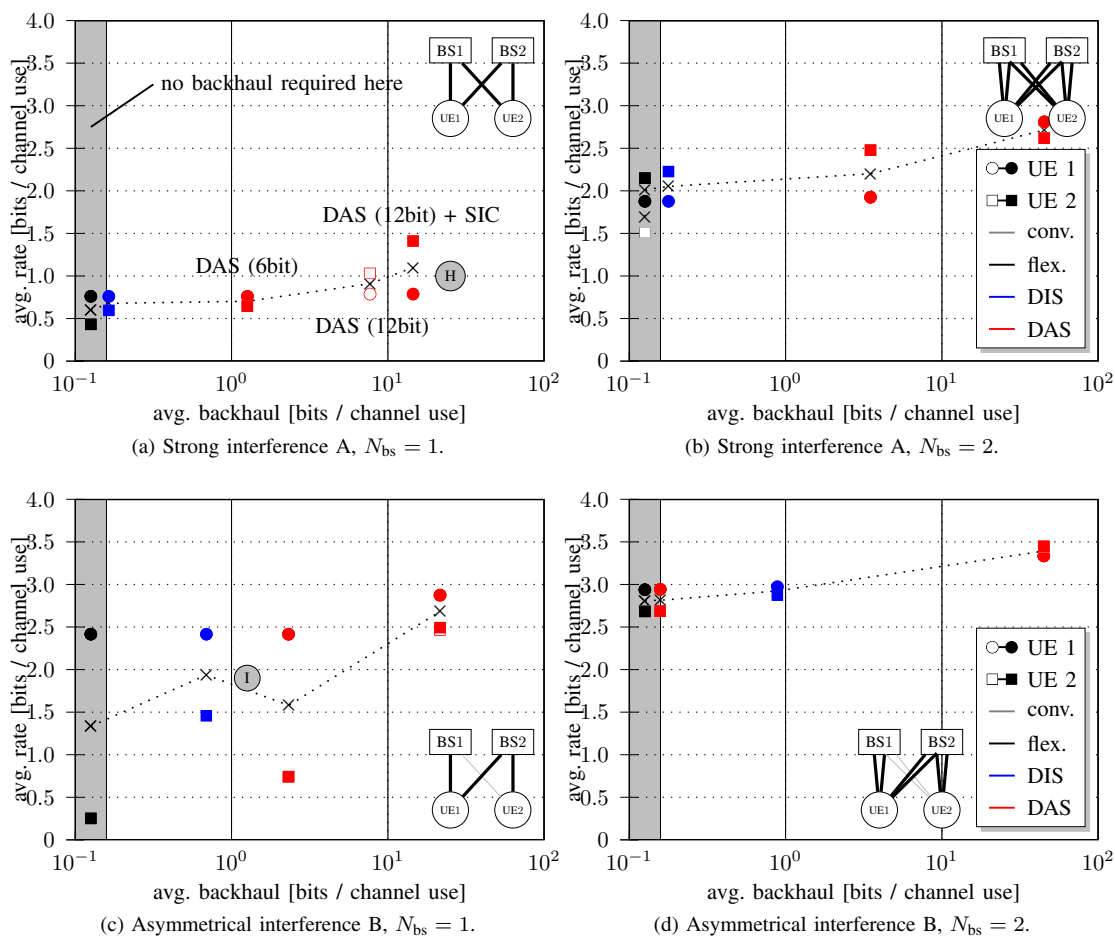


Fig. 5: Trade-off between average rates and required backhaul.

#### ACKNOWLEDGEMENT

We would like to thank the project partners for the great collaboration and the German Ministry for Education and Research (BMBF) for the partial funding of project EASY-C. Further, this work would not have been possible without the support from Vincent Kotsch, Eckhard Ohlmer, Zhijun Rong, Jan Wulfes, Matthias Pötschke and Joachim Heft.

#### REFERENCES

- [1] W. McCoy, "Overview of 3GPP LTE Physical Layer: White Paper by Dr. Wes McCoy," *White Paper*, 2007.
- [2] P. Marsch, S. Khatkhat, and G. Fettweis, "A Framework for Determining Realistic Capacity Bounds for Distributed Antenna Systems," in *Proc. of the IEEE Information Theory Workshop (ITW'06)*, Oct. 2006.
- [3] S. Venkatesan, "Coordinating base stations for greater uplink spectral efficiency in a cellular network," in *Proc. of the Personal, Indoor and Mobile Radio Communications Conference (PIMRC'07)*, Sept. 2007.
- [4] M. Schellmann and V. Jungnickel, "Multiple CFOs in OFDM-SDMA Uplink: Interference Analysis and Compensation," *EURASIP Journal on Wireless Communications and Networking*, vol. 2009, 2009.
- [5] L. Maniatis, T. Weber, A. Sklavos, and Y. Liu, "Pilots for joint channel estimation in multi-user OFDM mobile radio systems," in *ISSSTA*, 2002.
- [6] P. Marsch and G. Fettweis, "A Framework for Optimizing the Uplink Performance of Distributed Antenna Systems under a Constrained Backhaul," in *Proc. of the IEEE International Conference on Communications (ICC'07)*, June 2007, pp. 975–979.
- [7] —, "On Uplink Network MIMO under a Constrained Backhaul and Imperfect Channel Knowledge," in *Proc. of the IEEE International Conference on Communications (ICC'09)*, June 2009.
- [8] R. Irmer, H.-P. Mayer, A. Weber, V. Braun, M. Schmidt, M. Ohm, N. Ahr, A. Zoch, C. Jandura, P. Marsch, and G. Fettweis, "Multisite field trial for LTE and advanced concepts," *IEEE Comm. Mag.*, 2009.
- [9] M. Grieger, P. Marsch, Z. Rong, and G. Fettweis, "Field Trial Results for a Coordinated Multi-Point (CoMP) Uplink in Cellular Systems," in *International ITG Workshop on Smart Antennas 2010*, Bremen, Germany, Feb. 2010, pp. 93–98.
- [10] R. Chundury, "Mobile broadband backhaul: Addressing the challenge," *Ericsson Review*, vol. 3, pp. 4–9, 2008.
- [11] P. Marsch and G. Fettweis, "On the Rate Region of a Multi-Cell MAC under Backhaul and Latency Constraints," in *Proc. of the Wireless Communications and Networking Conference (WCNC'08)*, March 2008.
- [12] V. Jungnickel, T. Wirth, M. Schellmann, T. Haustein, and W. Zirwas, "Synchronization of cooperative base stations," in *Proc. ISWCS*, 2008.
- [13] R. Shafik, S. Rahman, R. Islam, and N. Ashraf, "On the error vector magnitude as a performance metric and comparative analysis," in *Proc. of the International Conference on Emerging Technologies (ICET'06)*.
- [14] P. Marsch and G. Fettweis, "Uplink CoMP under a Constrained Backhaul and Imperfect Channel Knowledge," 2010, subm. to IEEE Trans. on Wirel. Comms. See <http://arxiv.org/abs/1002.3356>.
- [15] S. Kay, *Fundamentals of statistical signal processing: estimation theory*, 1993, vol. 1.
- [16] P. Marsch, P. Rost, and G. Fettweis, "Application Driven Joint Uplink-Downlink Optimization," in *ITG/IEEE Workshop on Smart Antennas (WSA'10)*, February 2010.
- [17] P. Marsch and G. Fettweis, *Coordinated Multi-Point under a Constrained Backhaul and Imperfect Channel Knowledge*, 2010, Ph.D. thesis.